Interplanetary Type III Burst Directivity in Anisotropic Turbulence

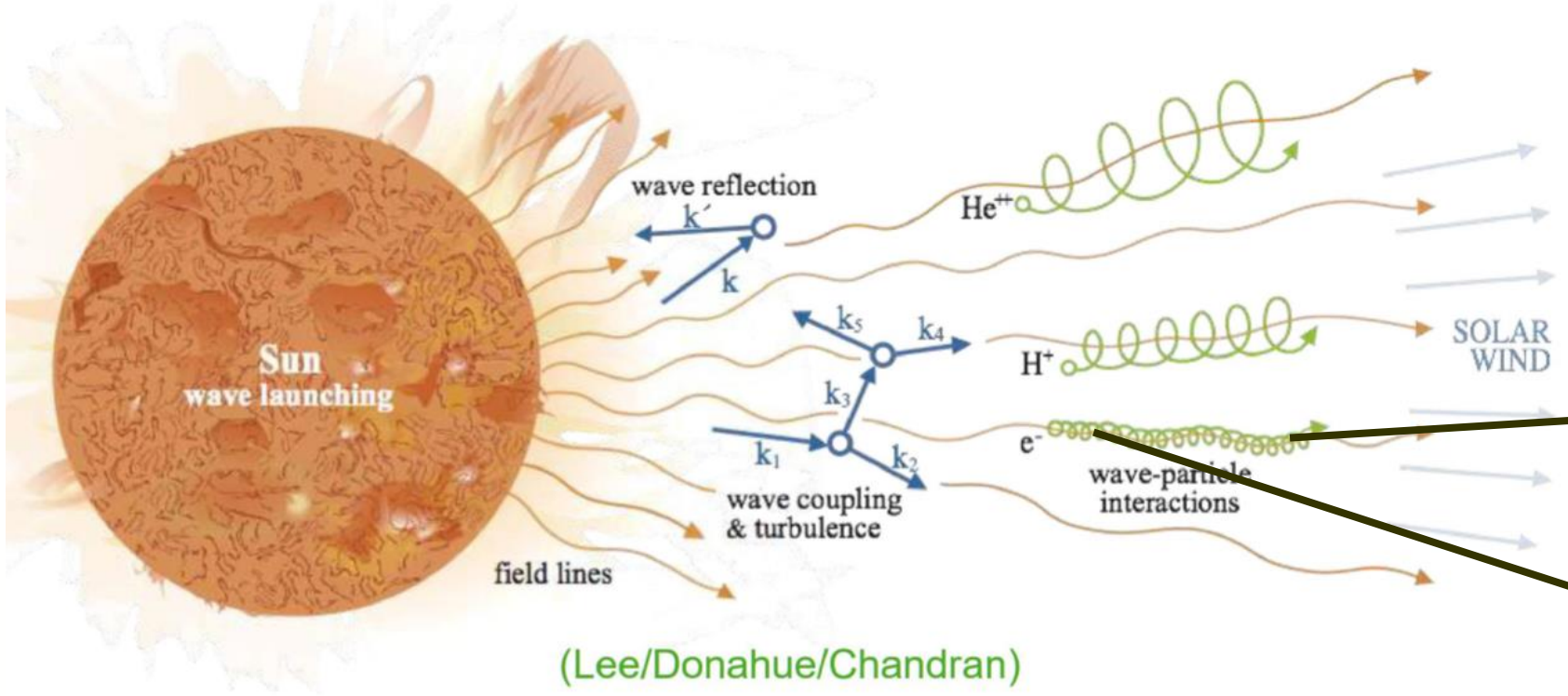
Daniel L. Clarkson, Eduard P. Kontar, Nicolina Chrysaphi

26 - 29 Feb 2024

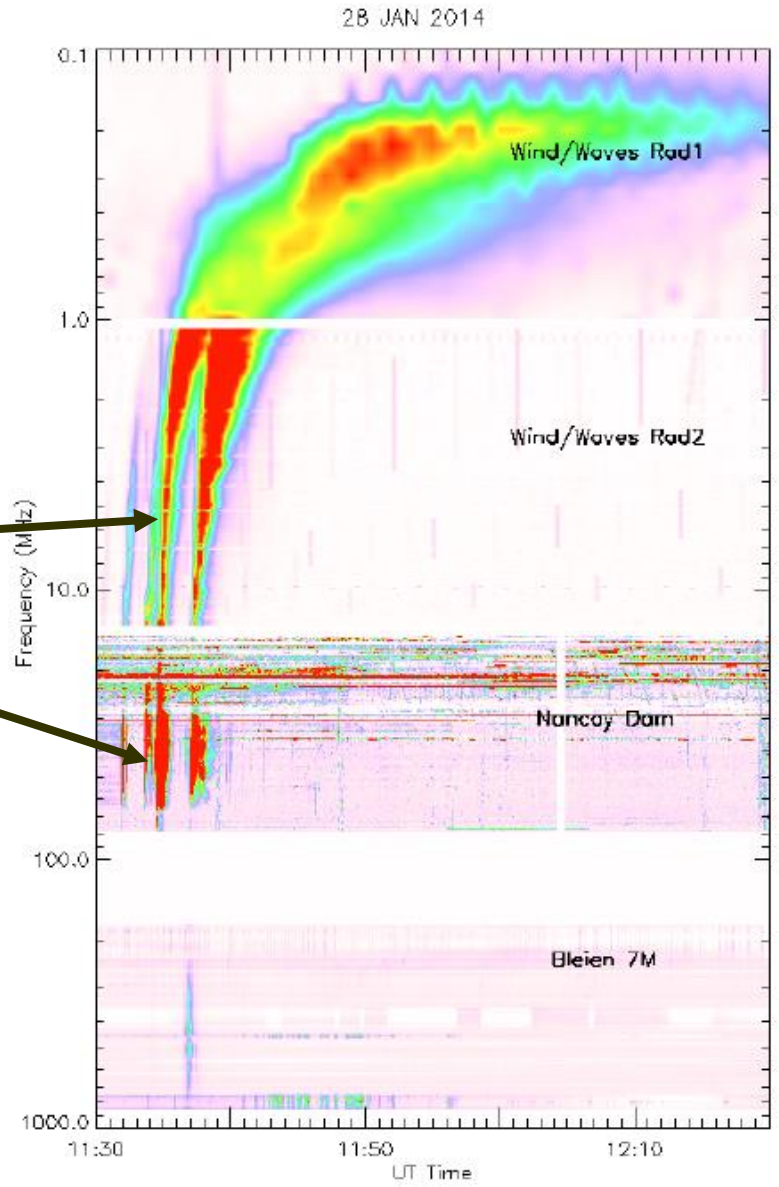
University of Glasgow, UK

Daniel.Clarkson@glasgow.ac.uk

Turbulent, Magnetised Environments



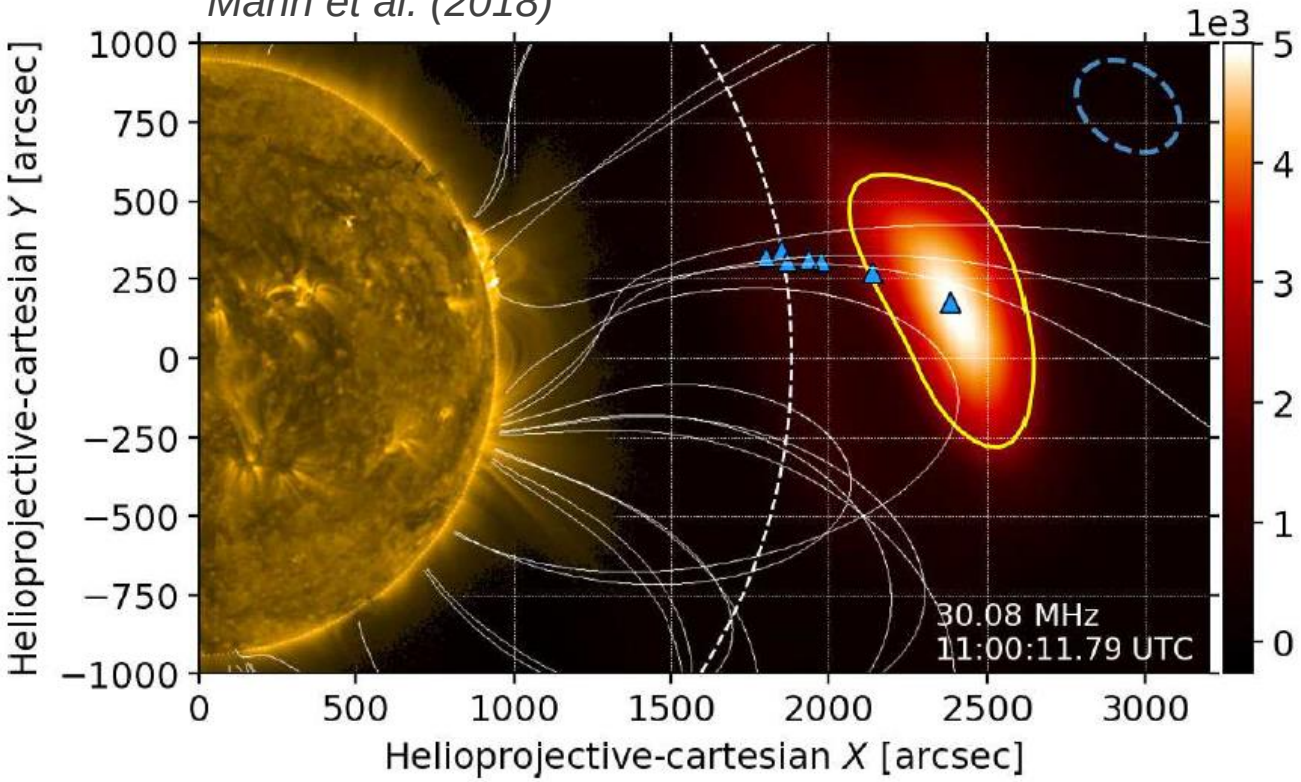
Type III Bursts

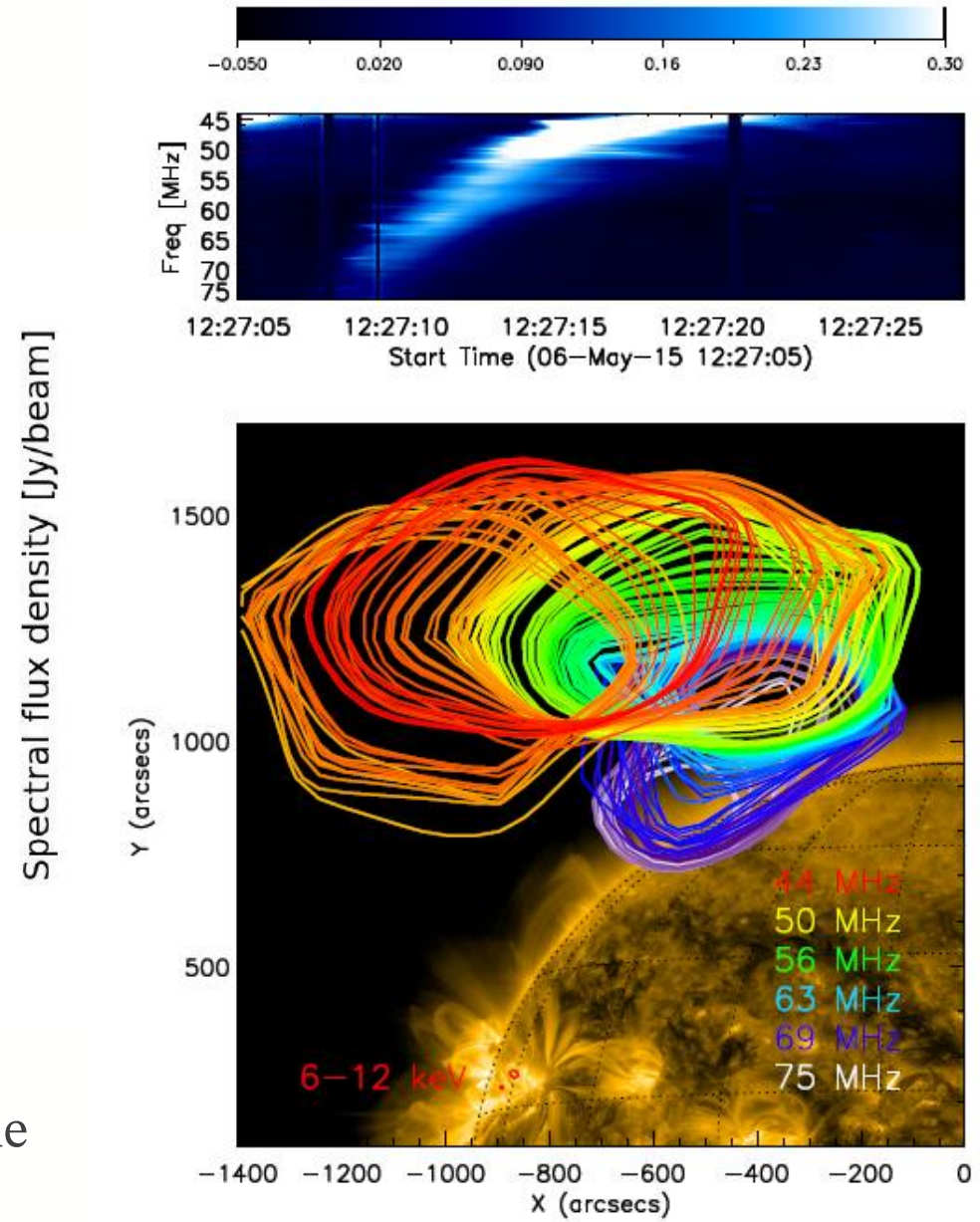


- Magnetic fluctuations, Density fluctuations, Velocity fluctuations

Tracing the Magnetic Field

Mann et al. (2018)

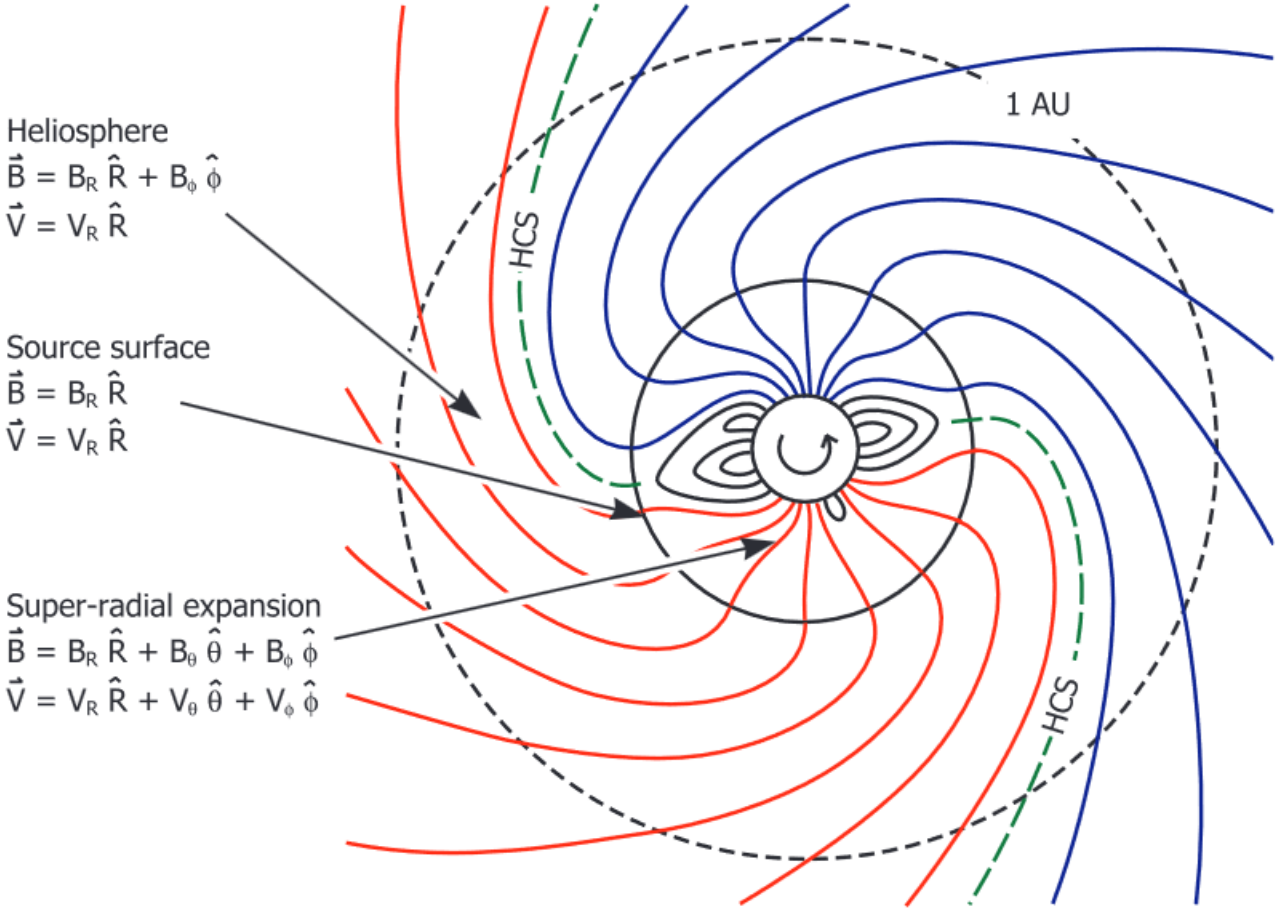




- Radio imaging can trace the motion of the emitting along the magnetic field close to the Sun.
- Imaging observations are not yet possible below ~20 MHz.

Reid et al. (2017)

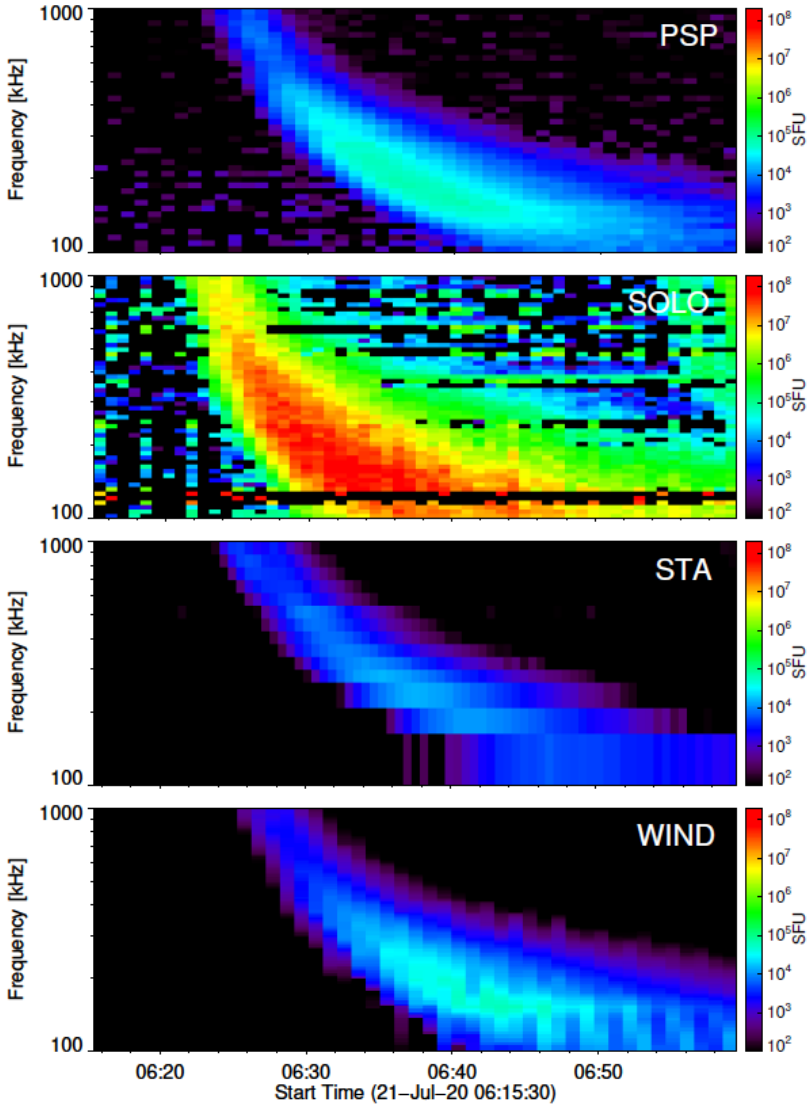
Heliospheric Magnetic Field

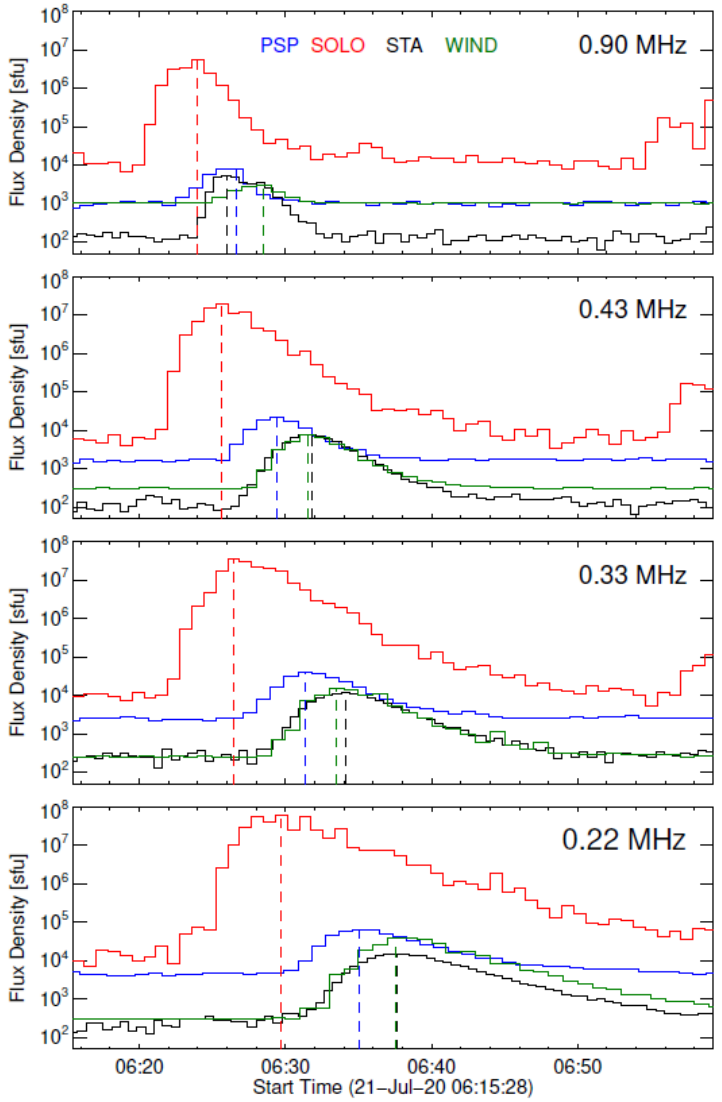


Owens & Forsyth (2013)

- Below ~1 MHz, ambient magnetic field follows Parker spiral
- In the ecliptic plane, magnetic field angle to radial direction is $\psi \simeq -\tan^{-1}(\Omega r / v_{\mathrm{sw}})$
- For $v_{\mathrm{sw}} = 400\ \mathrm{km\ s^{-1}}$, $\psi \approx 45°$
- Typical solar wind speeds vary between $340 - 420\ \mathrm{km\ s^{-1}}$ *(e.g. Larroderra & Cid, 2020)*
- 1 au ecliptic Heliospheric magnetic field measured by numerous spacecraft (Helios, Pioneer, Voyager) and now by Parker Solar Probe and Solar Orbiter <1 au.

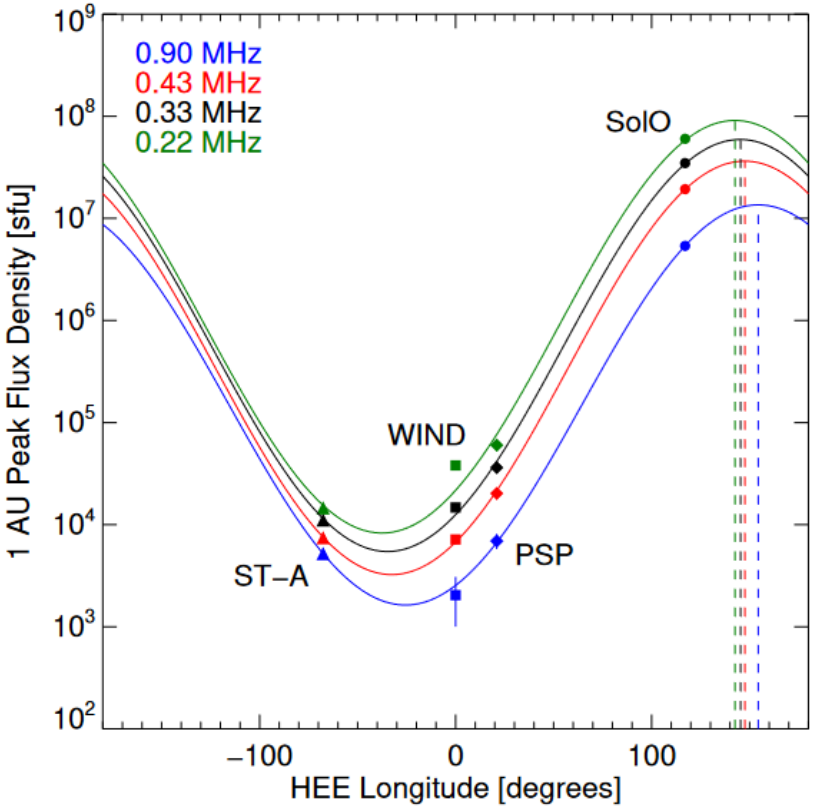
Multi-spacecraft Radio observations



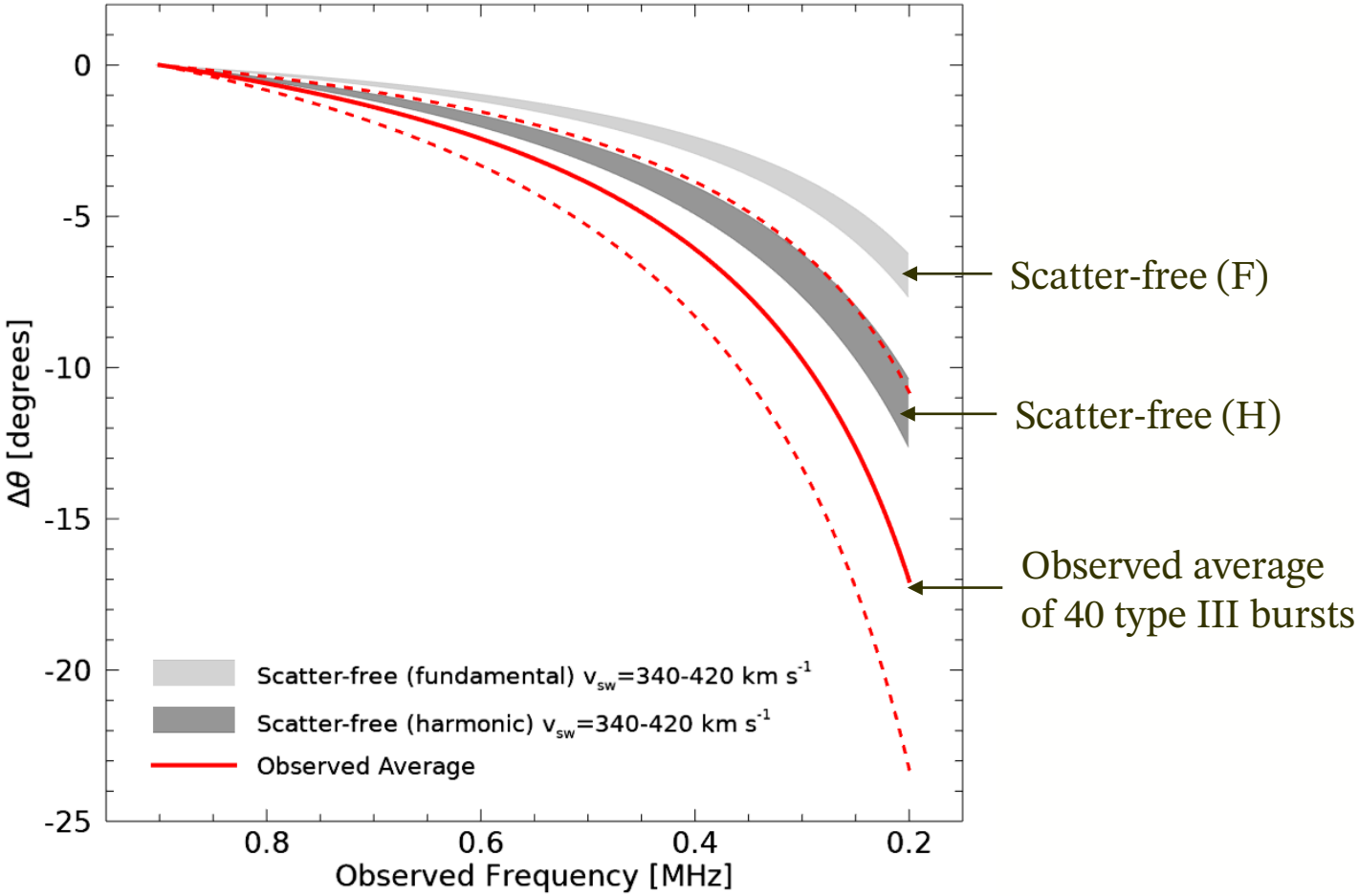


$$I = I_0 \exp\left(-\frac{1-\mu}{\Delta\mu}\right),$$

$$\mu = \cos(\theta_{sc} - \theta_0)$$



Peak Intensity Angular Deviation

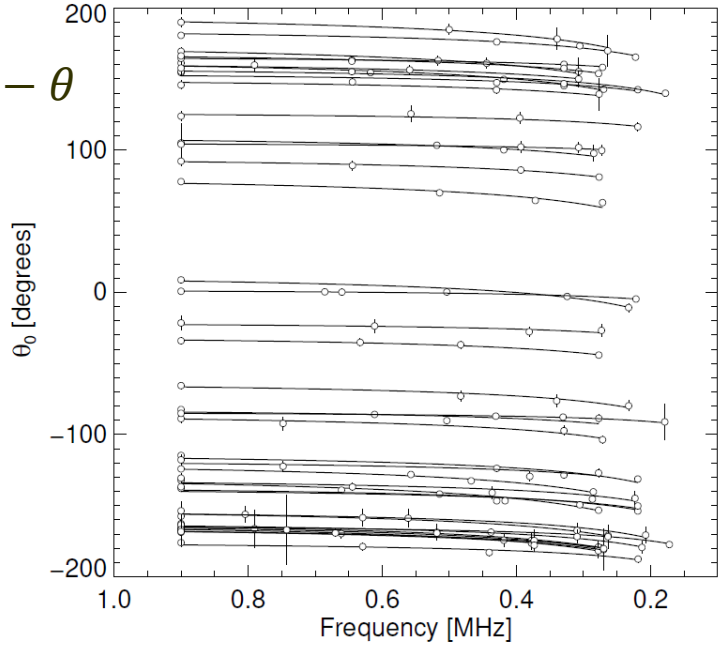


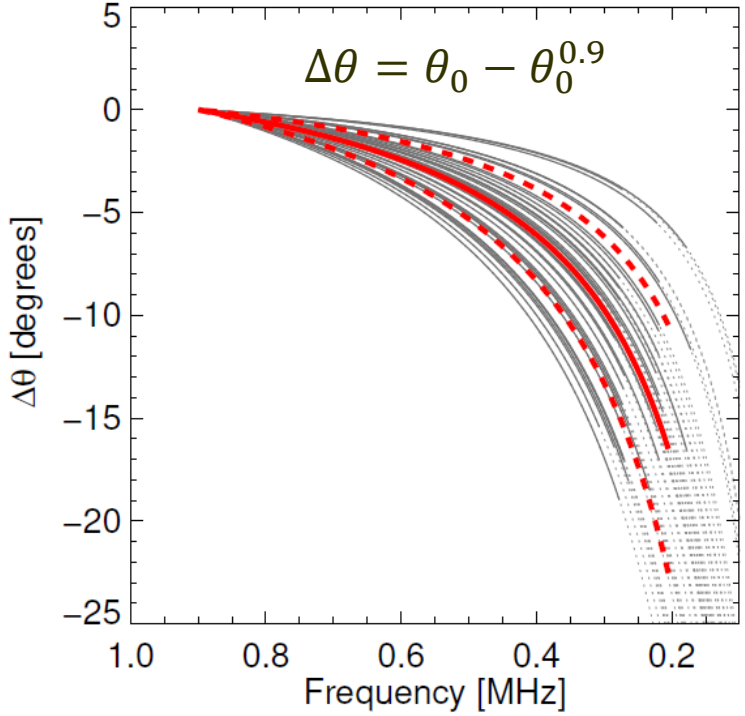
Scatter-free (F)

Scatter-free (H)

Observed average of 40 type III bursts

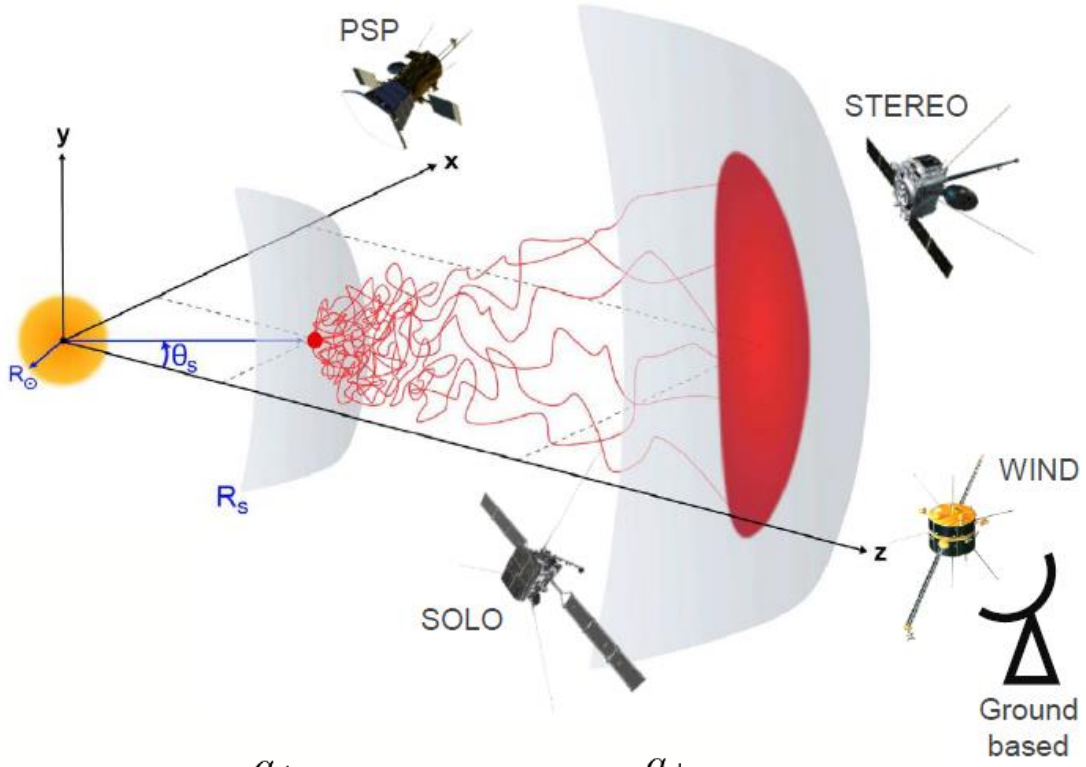
Fit: $\theta_0 = \frac{\gamma}{f} - \theta$

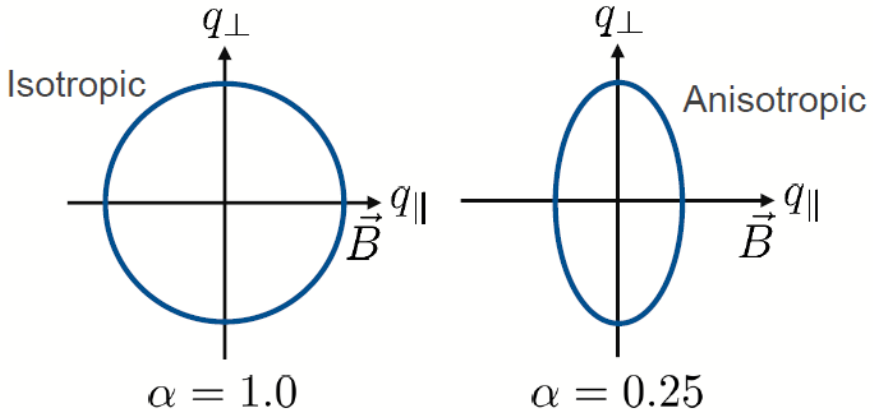




- Average observed shift from peak intensity fitting is larger than the scatter-free case in the emitting region.
- Requires an additional mechanism!

Anisotropic Density Fluctuations





Refractive index varies as $n_{\mathrm{ref}} = \left(1 - \frac{\omega_{\mathrm{pe}}^2}{\omega^2}\right)^{1/2}$

- Strong scattering near the emitting region

Field-aligned density fluctuations – elongated along magnetic field direction

Anisotropic radio-wave scattering acts to shift the apparent position of the source in the direction of the local magnetic field (*Kontar+2017, 2019*)

Turbulence profile modelled by *Kontar+2023* as:

$$\nu_s \propto \overline{q\epsilon^2}(r) = 2 \times 10^3 \alpha \left(1 - \frac{R_\odot}{r}\right)^{2.7} \left(\frac{R_\odot}{r}\right)^{0.7}$$

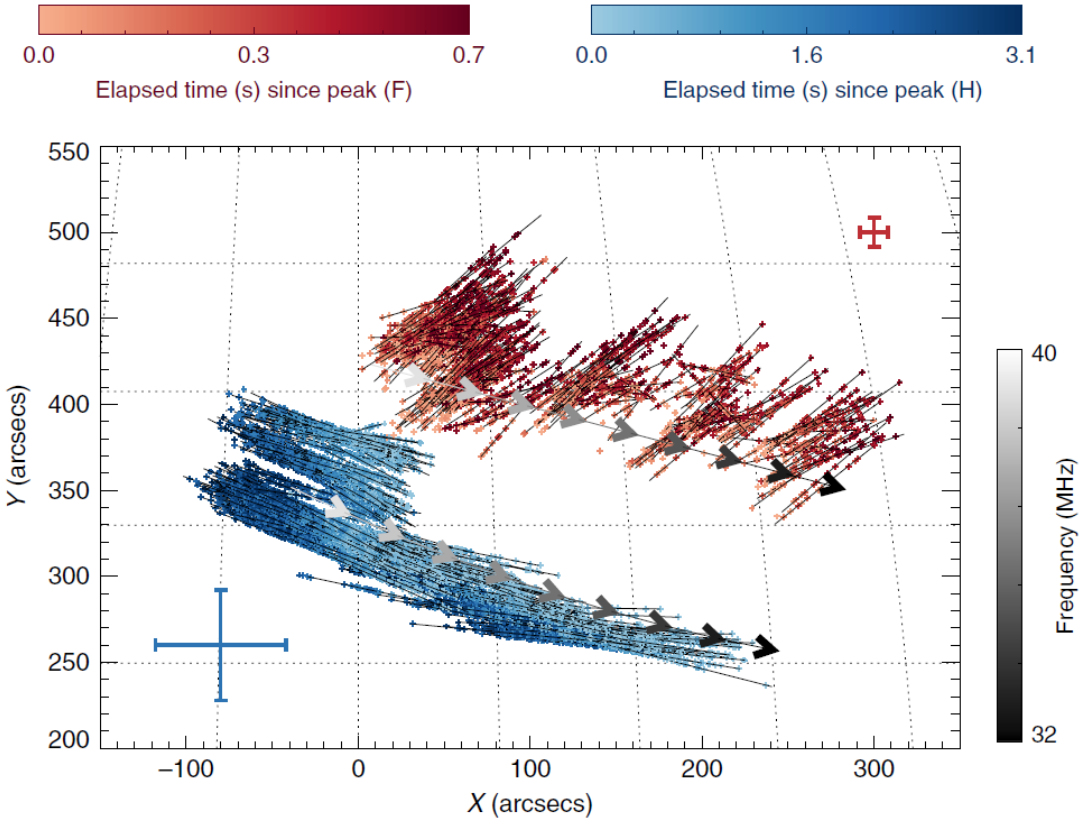
$$\alpha = \frac{q_\parallel}{q_\perp} = 0.25 - 0.4$$

Consistent with:

- Solar radio burst observations
- Radio point-sources observed through the solar atmosphere
- In-situ density turbulence

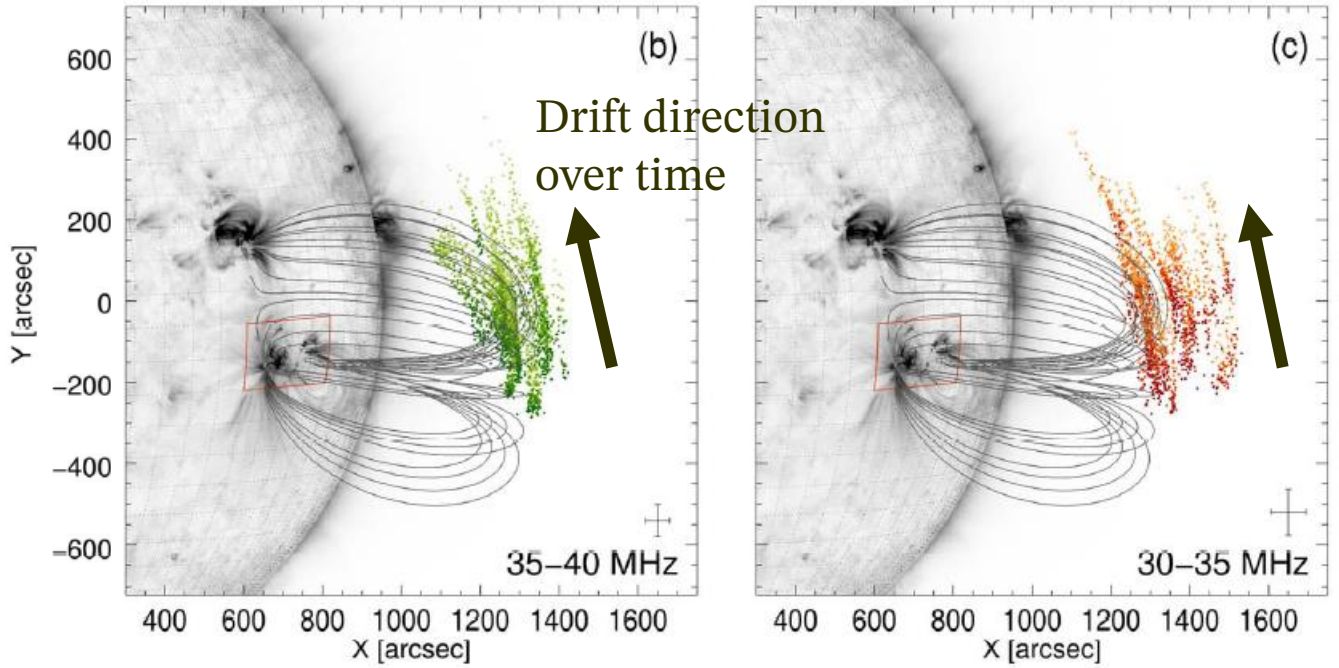
Radio-wave Channeling Along Field-lines

Type IIIb Striae Centroids



Kontar et al. (2017)

Radio Spikes Centroids

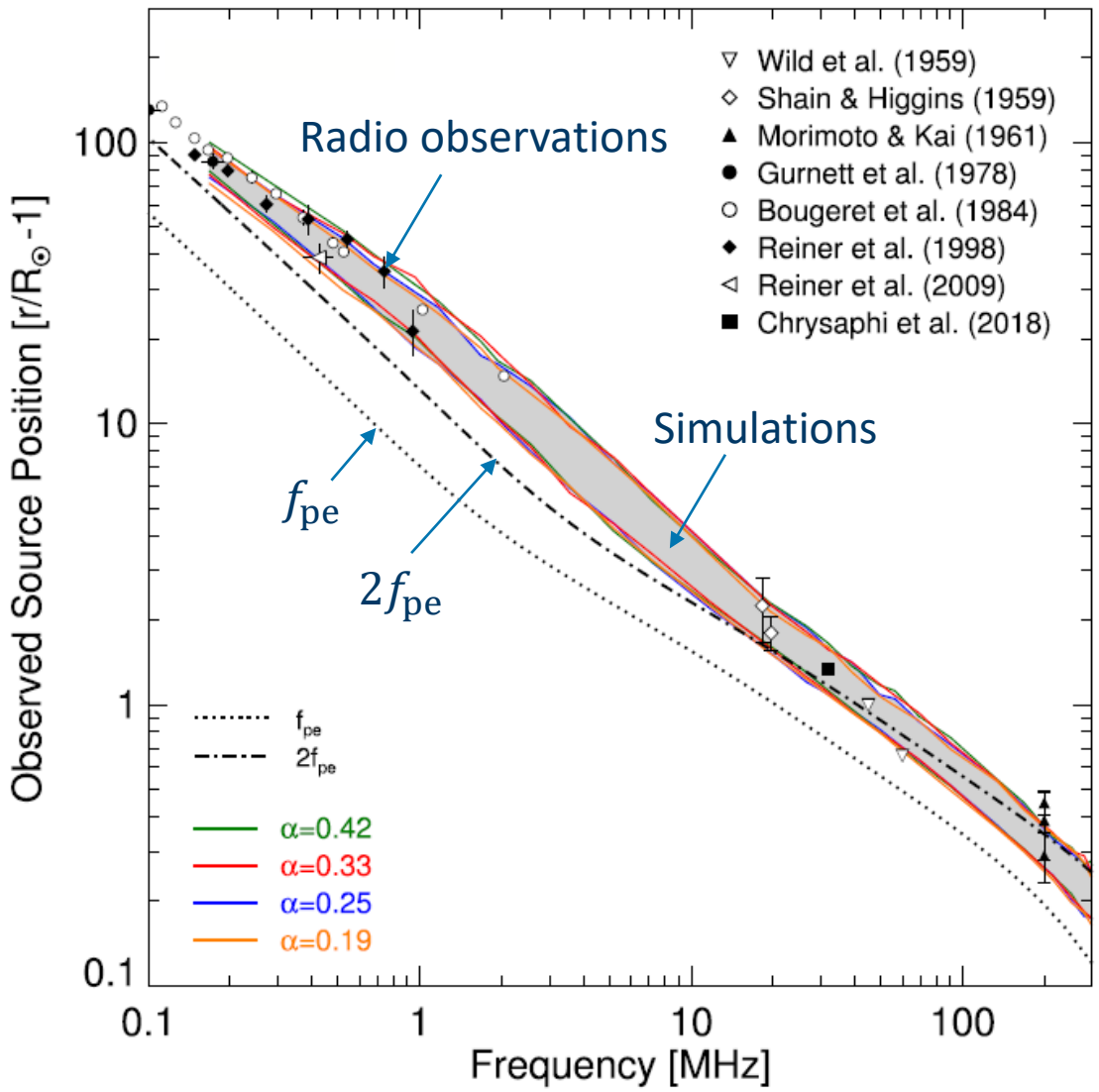


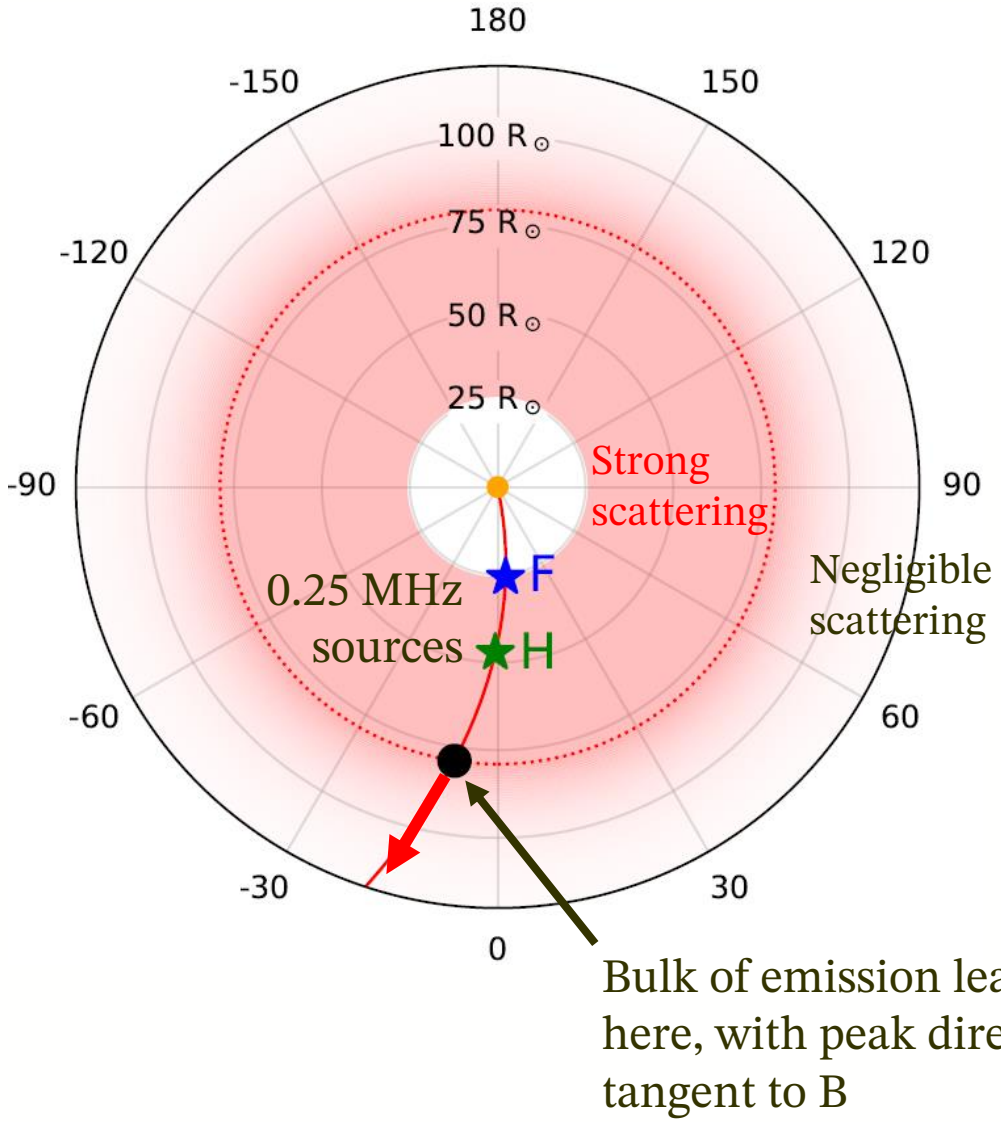
Clarkson et al. (2023)

Apparent Source Positions

- Both fundamental & harmonic emission are shifted to the same apparent position for a given frequency.
- Fundamental is shifted further than the harmonic.

Kontar et al. (2023)

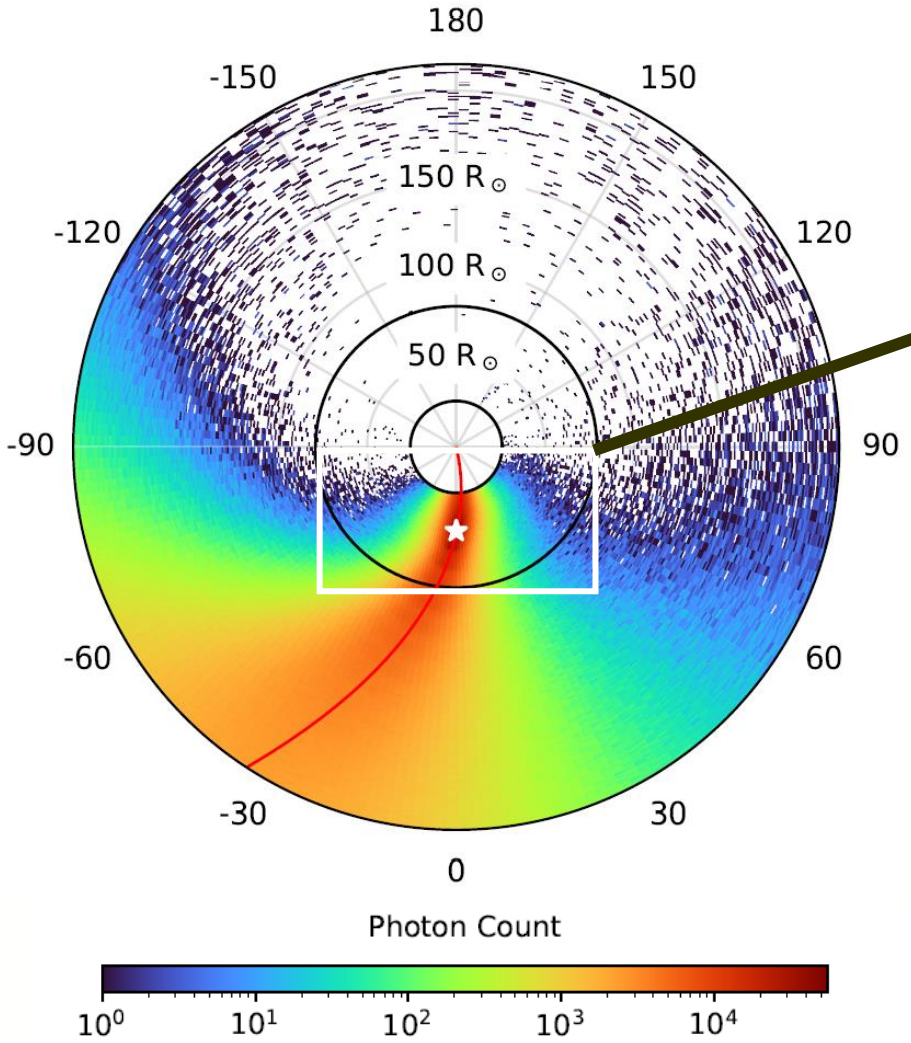


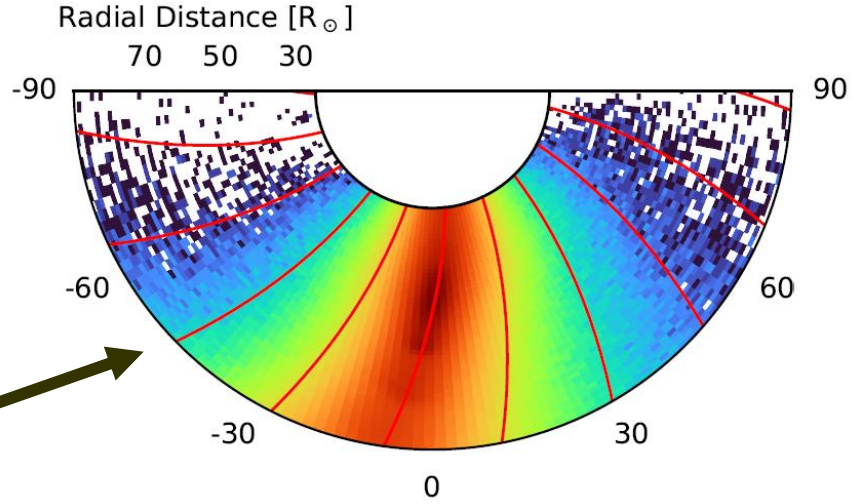


Anisotropic Scattering Simulations

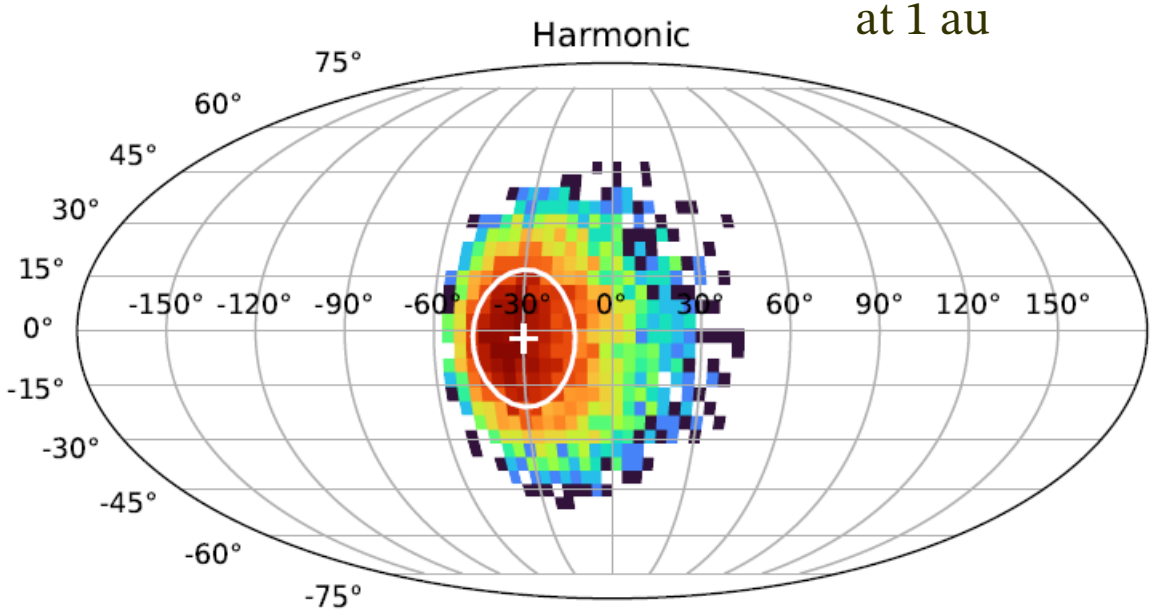
- Kontar+(2019, 2023) code
- 10^6 photons injected as a point source with initially isotropic wavevector distribution

All photon positions



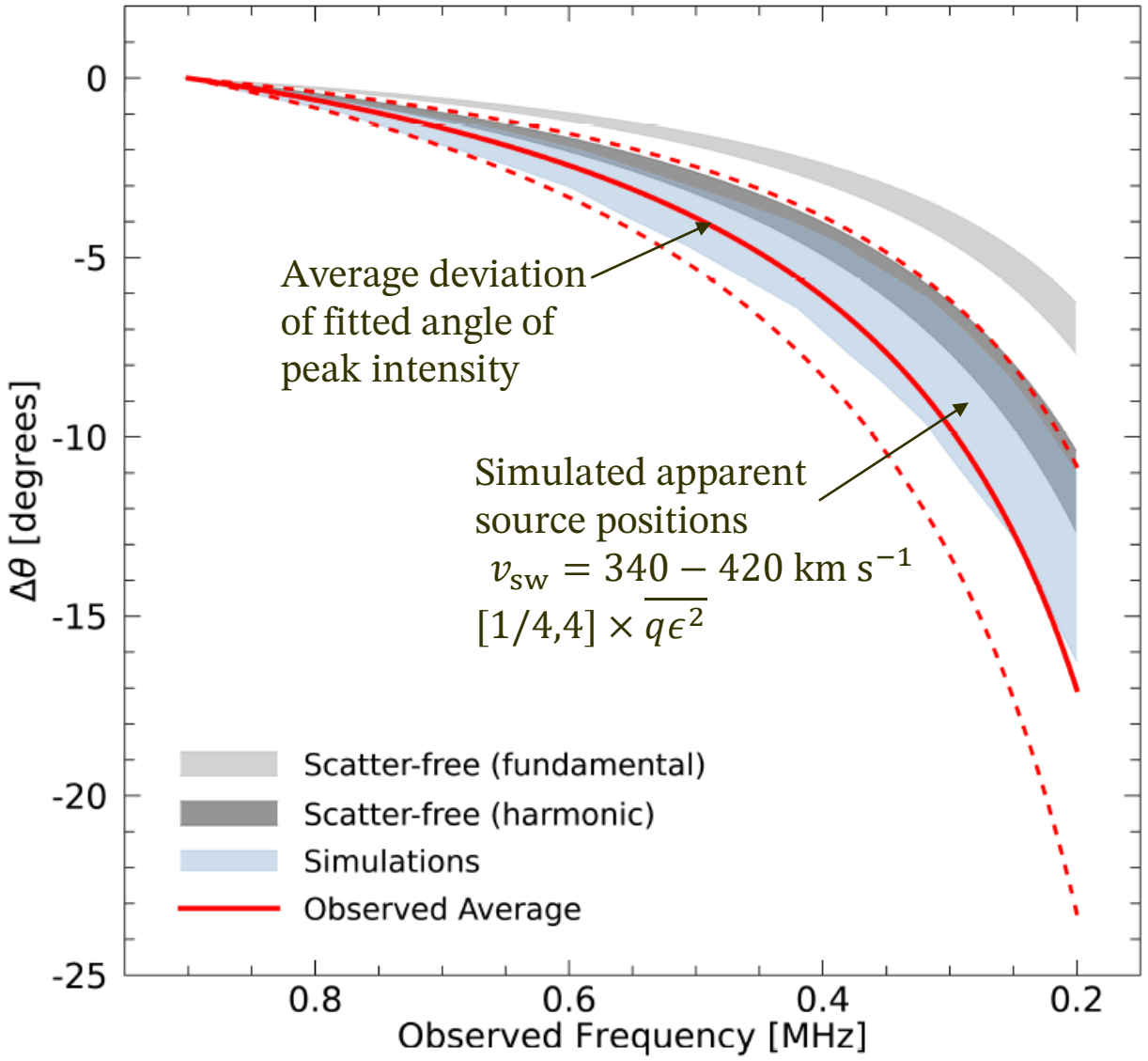


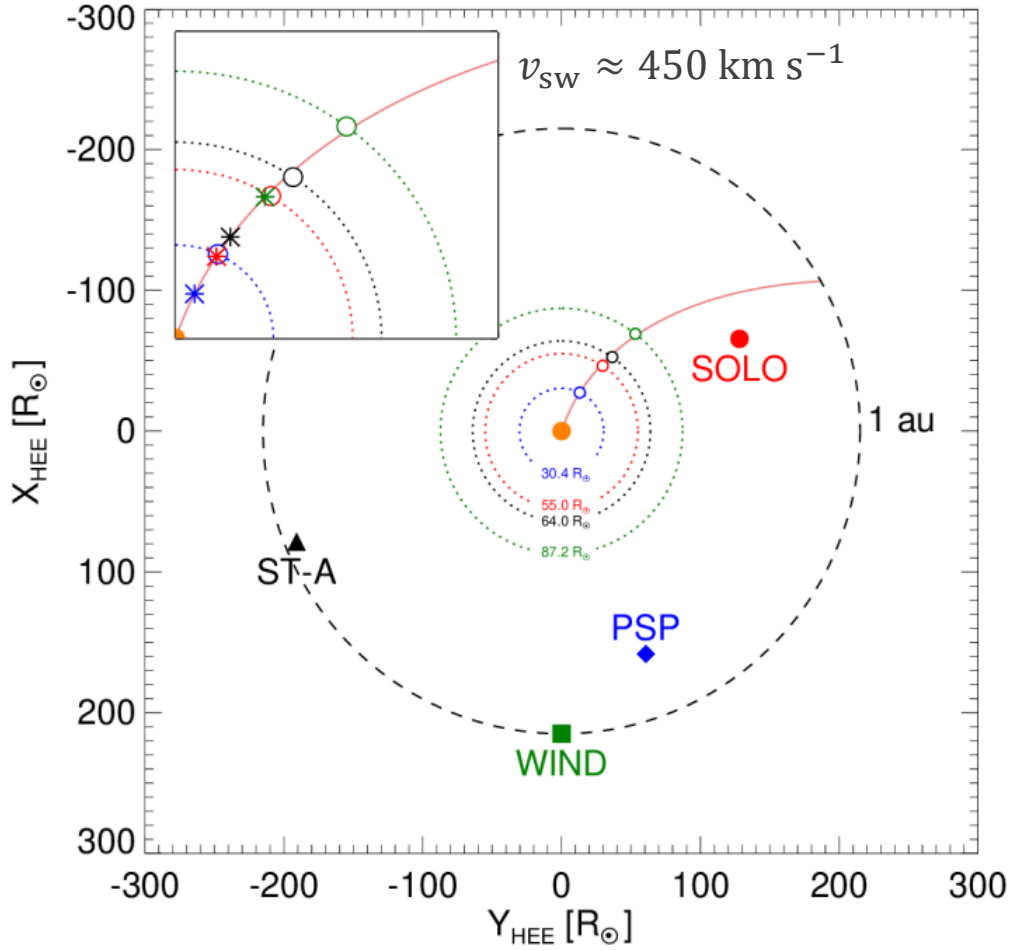
Peak intensity at 1 au



Magnetic Field Deviation

- Scattering simulations are consistent with the observed shift in the fitted peak intensity angle with decreasing frequency.
- The fitted peak intensity angles can reveal the magnetic structure following the anisotropic scattering theory.
- Intensity fitting can reveal the structure of magnetic field at the 'radius of last scattering'.





Summary

- Electrons propagate along field lines and emit radio emission that is then channelled further along the field line due to anisotropic density fluctuations.
- Observers will receive emission that is shifted away from the emitter location in the direction of the magnetic field curvature.
- Multi-spacecraft observations of type III radio bursts between 0.9-0.2 MHz can reveal the angular variation of the Parker spiral out to ~80-90 $R_{\odot}$.
- Radio observations offer a new diagnostic for inferring the magnetic field structure in any turbulent and magnetised astrophysical environment.